ACS OMEGA

Open Access



http://pubs.acs.org/journal/acsodf

Article

# Quantum Mechanical Spectral Analysis and Aldose Reductase Inhibition Evaluation of Synthetic New Pyrrolopyrazinones

Yun-Seo Kil, Junhyeung Park, Byeong-Seon Jeong, Punam Thapa, Young Jun Ok, Hyukjae Choi, Jee-Heon Jeong,* and Joo-Won Nam*

Cite This: *ACS Omega* 2025, 10, 13185−13192

Read Online

ACCESS | Metrics & More | Article Recommendations | Supporting Information

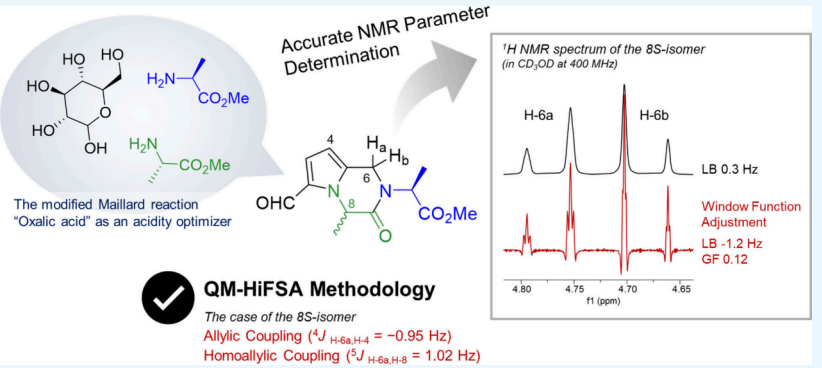


**ABSTRACT:** The Maillard reaction, known as the condensation of reduced sugars with amino acids, can be a great source of pyrroles for the discovery of bioactive compounds. In the present study, using glucose and L-alanine, two new pyrrolopyrazinones (**1a** and **1b**) were obtained. Subsequently, two more new pyrrolopyrazinones (**2a** and **2b**) were prepared by further hydrolyzing the methyl ester into carboxylic acid. The structures of the pyrrolopyrazinones were determined by interpretation of 1D and 2D NMR and HRESIMS data as well as computational calculation of ECD Cotton effects. Moreover, the broad $^{1}$H NMR peak shapes observed in the pyrrolopyrazinones were accurately resolved to the presence of long-range couplings, including allylic $^{4}J$ and homoallylic $^{5}J$ couplings, by employing quantum mechanics-driven $^{1}$H iterative full spin analysis (QM-HiFSA). The four pyrrolopyrazinones were evaluated for their biological efficacy in the treatment of diabetes in terms of their structural elements, including carboxyl functional groups. As a result, all four compounds were found to be moderately effective in inhibiting aldose reductase and also in proliferating mesenchymal stem cells.

## 1. INTRODUCTION

Pyrrole-based alkaloids have been a great pharmaceutical resource and further cyclization to the pyrrole core has broadened their chemical and therapeutic spectra.[1] Among their varieties, pyrrolopyrazinone contains one more cyclic system bearing an internal amide group. Natural pyrrolopyrazinones including logamides A−F, mukanadin C, and angelastin A were previously reported with various biological effects such as anticancer, antibacterial, and antifungal activities.[2−6] The pharmacological significance of the pyrrolopyrazinones has attracted total synthesis attempts.[7−9] Synthetic optimization, starting with the known pyrrolopyrazinones, has also been attempted to maximize their therapeutic efficacy.[10]

Diabetes can be simply described by the common feature of high blood glucose, but its management is not straightforward as it can lead to complications. When blood glucose levels are elevated, glucose metabolism is activated to deal with the excess glucose. The polyol pathway is one of the main mechanisms for regulating blood glucose levels, but it also leads to the overproduction of sorbitol, fructose, and NADH. Subsequently, sorbitol accumulation causes osmotic stress and cell membrane damage.[11] NADH/NAD+ redox imbalance also plays an important role in the development of diabetic complications due to oxidative stress and damage.[12] In this regard, aldose reductase has emerged as a crucial pharmacological target in diabetes treatment, as it is the rate-limiting enzyme of the polyol pathway.[13,14] To date, the development of small molecule aldose reductase inhibitors has unveiled effective substances with a variety of structural features, with the presence of a carboxylic acid functional group considered to be the most critical feature.[15−17]

**Received:** November 25, 2024
**Revised:** February 20, 2025
**Accepted:** March 18, 2025
**Published:** March 26, 2025

Table 1. $^{1}$H (400 MHz) and $^{13}$C NMR (100 MHz) Data of Compounds 1a and 1b in $CD_3OD$[a]

| | $\delta_H$ ($J$ in Hz) | | | | $\delta_C$ | |
|---|---|---|---|---|---|---|
| | 1a | | 1b | | | |
| position | Manual analysis | QM-HiFSA analysis | Manual analysis | QM-HiFSA analysis | 1a | 1b |
| 1 | 9.43, s | 9.4299, d (−0.17) | 9.43, s | 9.4293, d (−0.15) | 180.5, CH | 180.5, CH |
| 2 | - | - | - | - | 131.5, C | 131.5, C |
| 3 | 7.12, d (4.1) | 7.1193, dddd (4.09, 0.35, 0.21, −0.17) | 7.11, d (4.1) | 7.1106, dddd (4.08, 0.27, 0.25, −0.15) | 127.1, CH | 127.0, CH |
| 4 | 6.24, br d (4.1) | 6.2449, dddd (4.09, −0.95, −0.57, 0.31) | 6.26, br d (4.1) | 6.2553, dddd (4.08, −0.95, − 0.57, 0.32) | 107.9, CH | 108.0, CH |
| 5 | - | - | - | - | 134.8, C | 134.8, C |
| 6 | 4.77, br d (16.5) | 4.7687, dddd (−16.45, 1.03, − 0.95, 0.35) | 4.73, d (16.5) | 4.7181, dddd (−16.49, −0.57, 0.52, 0.25) | 43.4, $CH_2$ | 41.2, $CH_2$ |
| | 4.68, d (16.5) | 4.6866, dddd (−16.45, −0.57, 0.54, 0.21) | 4.67, br d (16.5) | 4.6807, dddd (−16.49, 1.02, − 0.95, 0.27) | | |
| 7 | - | - | - | - | 170.3, C | 170.9, C |
| 8 | 5.54, br q (7.0) | 5.5384, qddd (7.00, 1.03, 0.55, 0.31) | 5.55, br q (7.0) | 5.5496, qddd (7.02, 1.02, 0.52, 0.32) | 56.5, CH | 56.5, CH |
| 9 | 1.57, d (7.0) | 1.5687, d (7.00) | 1.57, d (7.0) | 1.5731, d (7.02) | 20.1, $CH_3$ | 20.0, $CH_3$ |
| 10 | 4.87, q (7.3) | 4.8741, qd (7.31, 0.29) | 5.08, q (7.4) | 5.0755, qd (7.38, 0.27) | 55.6, CH | 54.2, CH |
| 11 | - | - | - | - | 172.8, C | 172.9, C |
| 12 | 1.55, d (7.3) | 1.5475, d (7.31) | 1.52, d (7.4) | 1.5161, d (7.38) | 14.6, $CH_3$ | 14.0, $CH_3$ |
| COO*Me* | 3.71, s | 3.7140, d (0.29) | 3.75, s | 3.7470, d (0.27) | 53.1, $CH_3$ | 53.1, $CH_3$ |

[a]Coupling constants less than 1 Hz determined by QM-HiFSA analysis were not apparently visible in the manual analysis, showing only line-broadening effects. Chemical shifts ($\delta$) and coupling constants ($J$) obtained from the QM-HiFSA were reported at 0.1 ppb and 10 mHz levels, respectively, upon the recommendation[19]

The proton ($^{1}$H) is one of the NMR active nuclei and is a fairly dominant isotope in nature (99.98%). As such, $^{1}$H NMR spectroscopy has been one of the most useful one-dimensional NMR techniques, further supported by the fact that hydrogen atoms are the main building blocks of organic compounds. Organic chemistry has taken advantage of obtaining structural information about molecules from chemical shifts ($\delta$) in $^{1}$H NMR spectra, which depend on the local chemical environment of a particular nucleus. The coupling constant ($J$) is a result of the spin interaction of the two nuclei and, together with the chemical shift, provides essential information for structure determination. However, manual interpretation of NMR data is rather limited for accurate determination of NMR parameters; therefore, a computational strategy, quantum mechanics-driven $^{1}$H iterative full spin analysis (QM-HiFSA) can be applied to address this issue. In QM-HiFSA analysis, replicas of the experimental spectra are first calculated, after which accurate NMR parameters, including chemical shifts, coupling constants, and line widths, are obtained as contained in the calculated spectra. The resulting accurate parameters will aid in structure determination and can be used for effective dereplication.[18−22]

In this study, new pyrrolopyrazinones were discovered in a modified Maillard reaction of glucose and L-alanine (L-Ala). Their structures were elucidated by interpreting 1D and 2D NMR and HRESIMS data as well as computationally calculating their ECD Cotton effects. QM-HiFSA was further performed to accurately extract small coupling constants from the $^{1}$H NMR spectra. In addition, structural characteristics as molecules containing carboxylic acid groups determined that they were suitable to be evaluated for aldose reductase inhibitory effects. Proliferative effects on mesenchymal stem cells were also tested to determine their potential for synergy in the treatment of diabetes-induced cell damage.[23]

## 2. EXPERIMENTAL SECTION

### 2.1. General Experimental Methods and Chemicals.

All reactions were monitored by thin-layer chromatographic (TLC) analyses using Silica gel 60 $F_{254}$ plates (aluminum sheets, Merck, Germany) with visualization under 254 and 365 nm UV light. The high-performance liquid chromatography coupled with a photo diode array and electrospray ionization mass spectrometry (HPLC-PDA-LRESIMS) data were also obtained for the reaction products before and after purification, using an Agilent 1260 series LC system coupled to a 6120 series single quadrupole mass spectrometer, with a Phenomenex Luna 3 $\mu$m $C_{18}$(2) column (100 Å, 150 × 4.6 mm), under a gradient elution condition consisting of 5% MeCN in $H_2O$ containing 0.05% HCOOH (A) and 100% MeCN containing 0.05% HCOOH (B) (5 → 100% B) at a flow rate of 0.7 mL/min. L-Alanine (L-Ala) and D-glucose were obtained from the Tokyo Chemical Industry (TCI, Tokyo, Japan). Thionyl chloride ($SOCl_2$) was from Duksan (Seoul, Korea). Anhydrous dimethyl sulfoxide (DMSO), oxalic acid, tetrahydrofuran (THF), $Et_3N$, and $LiOH{\cdot}H_2O$ were purchased from Sigma (Saint Louis, MO, USA). All other chemicals were also obtained commercially and used without any further purification. The reaction products were purified using silica gel open column chromatography (CC, 60 Å, 40−63 $\mu$m, Merck, Germany) and HPLC using a Waters HPLC system (Milford, CT, USA), with a YMC-Pack SIL (120 Å, 5 $\mu$m, 250 × 10.0 mm).

The optical rotation measurement was conducted on a JASCO P-2000 polarimeter (JASCO Co., Tokyo, Japan). The electronic circular dichroism (ECD) was recorded using a JASCO J-810 CD-ORD spectropolarimeter (JASCO Co., Tokyo, Japan), at the Core Research Support Center for Natural Products and Medical Materials (CRCNM). The 1D and 2D NMR experiments were performed on a Bruker AVANCE NEO spectrometer ($^{1}$H, 600 MHz, Oxford magnet, Bruker Switzerland AG, Fällanden, Switzerland) at the CRCNM, and a Bruker AVANCE DPX spectrometer ($^{1}$H,


https://doi.org/10.1021/acsomega.4c10696
ACS Omega 2025, 10, 13185−13192

400 MHz, Bruker Switzerland AG, Fällanden, Switzerland) at the College of Pharmacy, Yeungnam University, operated with Bruker TopSpin 4.1.3 software (Billerica, MA, USA). The HRESIMS data were acquired at the CRCNM using a Thermo Scientific Q Exactive Hybrid Quadrupole-Orbitrap mass spectrometer (Waltham, MA, USA).

**2.2. Synthesis of Methyl Esters 1a and 1b.** The modified Maillard reaction was performed after esterification of the substrate amino acid L-Ala as previously described.[24] To a suspension of L-Ala (510 mg, 5.7 mmol) in MeOH (10 mL), $SOCl_2$ (3 mL) was slowly added in an ice-bath. The mixture was stirred at room temperature overnight and then concentrated to afford L-H-Ala-OMe·HCl as a white powder (800 mg, 5.7 mmol, yield 100%). Next, the hydrochloride salt (78.7 mg, 0.57 mmol) was mixed with D-glucose (102.0 mg, 0.57 mmol) and $Et_3N$ (78.8 μL, 0.57 mmol) in anhydrous DMSO (0.75 mL) and was stirred at room temperature for 1 h. Oxalic acid (52.0 mg, 0.58 mmol) was added to the mixture, and it was stirred at 90 °C for another 1 h. The resulting reaction mixture was cooled to room temperature, quenched with water (5 mL), and then extracted with EtOAc (3 × 5 mL). The volatiles were removed from the combined organic solution under reduced pressure. Compounds **1a** (2.2 mg) and **1b** (2.6 mg) were obtained from the reaction product through silica gel column chromatography (hexanes/EtOAc, 8:2 to 6:4), followed by further purification using semipreparative HPLC (hexanes/EtOAc, 6:4), with elution at $t_R$ 25.6 and 21.8 min, respectively. The physical and spectral data of **1a** and **1b** are as follows:

*Methyl (S)-2-((S)-6-Formyl-4-methyl-3-oxo-3,4-dihydropyrrolo[1,2-a]pyrazin-2(1H)-yl)propanoate (**1a**).* Colorless amorphous solid; yield 1.5%; $[\alpha]_D^{20}$ + 21 (*c* 0.1, MeOH); UV (HPLC) $\lambda_{max}$ 286 nm; ECD (MeOH) $\lambda_{max}$ ($\Delta\varepsilon$) 230.2 (−0.73), 245.7 (−0.76), 292.4 (+1.01) nm; $^1$H (400 MHz) and $^{13}$C NMR data (100 MHz in $CD_3OD$), see Table 1; HRMS (ESI) *m*/*z* $[M + H]^+$ calcd. for $C_{13}H_{17}O_4N_2$ 265.1183, found 265.1178.

*Methyl (S)-2-((R)-6-Formyl-4-methyl-3-oxo-3,4-dihydropyrrolo[1,2-a]pyrazin-2(1H)-yl)propanoate (**1b**).* White amorphous solid; yield 1.7%; $[\alpha]_D^{20}$ − 72 (*c* 0.1, MeOH); UV (HPLC) $\lambda_{max}$ 286 nm; ECD (MeOH) $\lambda_{max}$ ($\Delta\varepsilon$) 235.1 (+1.15), 251.1 (+1.10), 292.5 (−1.57) nm; $^1$H (400 MHz) and $^{13}$C NMR data (100 MHz in $CD_3OD$), see Table 1; HRMS (ESI) *m*/*z* $[M + H]^+$ calcd. for $C_{13}H_{17}O_4N_2$ 265.1183, found 265.1178.

**2.3. Synthesis of Carboxylic Acids 2a and 2b.** For basic hydrolysis of ester group, starting compounds (2 mg, 0.0076 mmol, each) were dissolved in THF-$H_2O$ (1:1, 1 mL) together with $LiOH·H_2O$ (0.7 mg, 0.017 mmol) in an ice bath. The mixture was then stirred at room temperature for 2 h. After completion of the reaction, the resulting mixture was acidified to pH 1 ∼ 2 with 1 M HCl and partitioned against EtOAc (3 × 1 mL). The combined organic layers were concentrated under reduced pressure, and the products were purified by silica gel column chromatography (DCM/MeOH, 9:1 to 6:4). The physical and spectral data of **2a** and **2b** are as follows:

*(S)-2-((S)-6-Formyl-4-methyl-3-oxo-3,4-dihydropyrrolo[1,2-a]pyrazin-2(1H)-yl)propanoic Acid (**2a**).* Colorless amorphous solid; 1.7 mg, yield 90%; $[\alpha]_D^{20}$ + 13 (*c* 0.05, MeOH); ECD (MeOH) $\lambda_{max}$ ($\Delta\varepsilon$) 219.7 (−1.30), 251.0 (−0.69), 293.7 (+0.43) nm; $^1$H NMR ($CD_3OD$, 600 MHz): $\delta$ 9.40 (1H, s, H-1), 7.10 (1H, d, *J* = 4.1 Hz, H-3), 6.22 (1H, br d, *J* = 4.1 Hz, H-4), 5.53 (1H, br q, *J* = 7.0 Hz, H-8), 5.07 (1H, q, *J* = 7.4 Hz, H-10), 4.75 (1H, d, *J* = 16.4 Hz, H-6$\beta$), 4.66 (1H, br d, *J* = 16.4 Hz, H-6$\alpha$, stereospecifically assigned based on a NOE correlation of H-6$\alpha$/$H_3$-9, Figure S21, Supporting Information), 1.57 (3H, d, *J* = 7.0 Hz, $H_3$-10), 1.48 (3H, d, *J* = 7.4 Hz, $H_3$-12); $^{13}$C NMR ($CD_3OD$, 150 MHz): $\delta$ 180.3 (C-1), 178.1 (C-11), 170.0 (C-7), 135.7 (C-5), 131.3 (C-2), 127.3 (C-3), 107.8 (C-4), 56.5 (C-8), 55.7 (C-10), 41.4 (C-6), 20.3 (C-9), 15.7 (C-12); HRMS (ESI) *m*/*z* $[M + H]^+$ calcd. for $C_{12}H_{15}O_4N_2$ 251.1026, found 251.1022.

*(S)-2-((R)-6-Formyl-4-methyl-3-oxo-3,4-dihydropyrrolo[1,2-a]pyrazin-2(1H)-yl)propanoic Acid (**2b**).* colorless amorphous solid; 1.7 mg, yield 90%; $[\alpha]_D^{20}$ − 16 (*c* 0.05, MeOH); ECD (MeOH) $\lambda_{max}$ ($\Delta\varepsilon$) 235.1 (+0.58), 251.5 (+0.60), 298.1 (−0.70) nm; $^1$H NMR ($CD_3OD$, 600 MHz): $\delta$ 9.41 (1H, s, H-1), 7.10 (1H, d, *J* = 4.1 Hz, H-3), 6.23 (1H, br d, *J* = 4.1 Hz, H-4), 5.52 (1H, br q, *J* = 7.0 Hz, H-8), 5.04 (1H, q, *J* = 7.4 Hz, H-10), 4.80 (1H, br d, *J* = 16.9 Hz, H-6$\beta$, stereospecifically assigned based on a NOE correlation of H-6$\beta$/$H_3$-9, Figure S28, Supporting Information), 4.62 (1H, d, *J* = 16.9 Hz, H-6$\alpha$), 1.60 (3H, d, *J* = 7.0 Hz, $H_3$-10), 1.42 (3H, d, *J* = 7.4 Hz, $H_3$-12); $^{13}$C NMR ($CD_3OD$, 150 MHz): $\delta$ 180.4 (C-1), 178.0 (C-11), 170.4 (C-7), 136.0 (C-5), 131.4 (C-2), 127.2 (C-3), 107.7 (C-4), 56.7 (C-8), 55.8 (C-10), 40.5 (C-6), 19.9 (C-9), 15.4 (C-12); HRMS (ESI) *m*/*z* $[M + H]^+$ calcd. for $C_{12}H_{15}O_4N_2$ 251.1026, found 251.1022.

**2.4. Gaussian ECD Calculation.** Preliminary conformational searches were performed using the Merck molecular force field (MMFF) molecular mechanics model with an energy window of 10 kJ/mol in Spartan'18 (Wave function Inc., Irvine, CA, USA).[25] All conformers with a Boltzmann population >1% were selected and geometrically optimized by density functional theory (DFT) at the B3LYP/6-31G(d,p) level in the gas phase using Gaussian 16 software package (Gaussian Inc., Wallingford, CT, USA)[26] The optimized conformers representing greater than 1% of the Boltzmann population were submitted to ECD calculations by time-dependent DFT at the B3LYP/6-31+G(d,p) level with solvation of the polarizable continuum model (PCM) for MeOH in Gaussian 16. Boltzmann-averaged ECD spectra were generated using SpecDis 1.71.[27]

**2.5. Quantum Mechanics-Driven $^1$H Iterative Full Spin Analysis (QM-HiFSA).** HiFSA calculations were performed for **1a** and **1b** by using the CT (Cosmic Truth) software tool from NMR Solutions, Kuopio, Finland.[21] For the HiFSA calculations, the $^1$H NMR data (FIDs) were preprocessed using MestReNova 14.0.0 software (Mestrelab Research SL, Santiago de, Compostela, Spain) and saved in JCAMP-DX (.jdx) format: zero-filling to 256k, referencing to the residual solvent signal at $\delta_H$ 3.3100 ppm, baseline correction (fifth-order polynomial), manual phasing, and Lorentzian−Gaussian apodization (line broadening = − 0.1, Gaussian factor = 0.2). The 3D chemical structure MOL files were prepared using the MM2 energy minimization module in Chem 3D Ultra (ChemOffice 2020, PerkinElmer Informatics, Waltham, MA, USA).[24,28]

**2.6. Aldose Reductase Inhibition Test.** Aldose reductase inhibition capability of compounds was conducted using Aldose reductase Inhibition Screening Kit (Abcam, Cambridge, MA, USA) according to the manufacturer's instruction. Briefly, the compounds were first diluted in Assay Buffer to make 20× solutions of desired concentrations (25 and 50 μM). Next, 10 μL of compound solutions was mixed with 60 μL of NADPH Probe solution and 90 μL of Aldose Reductase


https://doi.org/10.1021/acsomega.4c10696
ACS Omega 2025, 10, 13185−13192

Scheme 1[a]

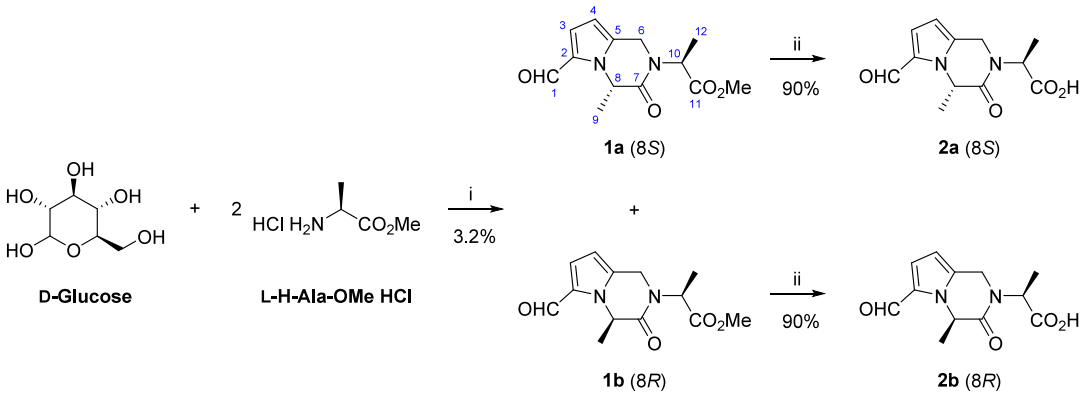


[a]Reagents and conditions: (i) $Et_3N$, DMSO, rt, 1 h then $(CO_2H)_2$, 90 °C, 1 h; (ii) LiOH, THF, $H_2O$, rt, 2 h.

Enzyme in the 96-well plate, which was incubated at 37 °C for 15−20 min. Then, 40 μL of Aldose Reductase Substrate solution was added to the reaction mixture in the wells. Absorbance of samples were immediately measured at 340 nm in a kinetic mode for 90 min using the microplate reader (SPARK 10M; TECAN, Switzerland). Relative Aldose reductase inhibition activity was calculated according to calculation formula provided in the product.

**2.7. Cell Proliferation Activity Test.** Human adipose-derived mesenchymal stem cells (hADMSCs, Passages 8−10; Epibiotech, Incheon, Republic of Korea) were cultured in the DMEM supplemented with 10% fetal bovine serum (Gibco, Grand Island, NY, USA) and 1% penicillin/streptomycin 100X (Hyclone Laboratories, South Logan, UT, USA). Cell proliferation activity was investigated using cell counting kit-8 assay (CCK-8 assay; Dojindo, Rockville, MD, USA). Briefly, hADMSCs were cultured in a 96-well plate at a density of 3000 cells/well for 24 h. After that, cells were treated with each of the four compounds at 50 μM for 48 h in an incubator (5% $CO_2$, 37 °C). After incubation period, 100 μL of CCK-8 reagent (5% in DMEM) was added to each well and incubated for 1 h at 37 °C. Then, the absorbance was measured at 450 nm using the microplate reader (SPARK 10M; TECAN, Switzerland). The relative cell viability was determined based on normalizing the absorbance of tested compounds to that of control cell group. Data statistical analysis was conducted by two-tailed unpaired *t* test using GraphPad Prism (Version. 8.4.2).

## 3. RESULTS AND DISCUSSION

**3.1. Synthesis and Structure Elucidation of Pyrrolo-pyrazinones.** The attempt at synthesis began with our previous metabolomics study, which showed that some of the radiation-bred mutants contained more pyrrole-2-carbaldehydes than the original species.[24] Since the occurrence of pyrrole-2-carbaldehyde can be related to the Maillard reaction of glucose and amino acids, synthetic preparations in the laboratory have also previously attempted to mimic naturally occurring conditions. Accordingly, they often require high temperatures for dehydration, as in baking and roasting processes. However, with the recent introduction of oxalic acid for optimal acidity by Adhikary et al., the harsh conditions of high reaction temperatures and long reaction times are no longer necessary.[29] Our synthetic attempts employed the modified Maillard reaction method to successfully obtain pyrrole-2-carbaldehydes, which were used as reference compounds for our previous NMR and MS-based metabolomics study.[24]

As part of the synthesis, a modified Maillard reaction was performed using D-glucose with L-alanine methyl ester hydrochloride (L-H-Ala-OMe·HCl) to obtain methyl 2-[2-formyl-5-(hydroxymethyl)-1*H*-pyrrol-1-yl]propanoate (2-PPA methyl ester).[24] This reaction also yielded a lactone-fused pyrrole compound, 4-methyl-3-oxo-3,4-dihydro-1*H*-pyrrolo-[2,1-*c*][1,4]oxazine-6-carbaldehyde, upon subsequent cyclization, as previously reported.[29] However, further review of the LC/LR-ESIMS data of the reaction product mixture revealed the presence of two additional product molecules, both observed with *m*/*z* values of 265.4 and 287.4 in the positive ionization mode, indicating a molecular weight of 264 (*m*/*z* 265.4 $[M + H]^+$, 287.4 $[M + Na]^+$). Thus, both products were expected as a result of one more equivalent introduction of the substrate, L-H-Ala-OMe (Scheme 1, a plausible mechanism for the formation in Figure S1, Supporting Information), and further chromatographic separation was performed to obtain the two molecules as pure compounds (**1a** and **1b**).

Compound **1a** was isolated as a colorless, amorphous solid, and the molecular formula was determined to be $C_{13}H_{16}O_4N_2$ based on the interpretation of its HRESIMS data ($[M + H]^+$ ion at *m*/*z* 265.1178, calcd 265.1183). The $^1H$ NMR spectrum of **1a** displayed characteristic signals of the 5-substituted pyrrole-2-carbaldehyde at $\delta_H$ 9.43 (1H, s, H-1), 7.12 (1H, d, *J* = 4.1 Hz, H-3), and 6.24 (1H, br d, *J* = 4.1 Hz, H-4) for the aldehyde and pyrrole, respectively, along with a pair of methylene proton signals at $\delta_H$ 4.77 (1H, br d, *J* = 16.5 Hz, H-6a) and 4.68 (1H, d, *J* = 16.5 Hz, H-6b) ("Manual analysis" in Table 1).[24,30] Moreover, two methine protons were observed as quartets, each coupled to a methyl group [$\delta_H$ 5.54 (1H, br q, *J* = 7.0 Hz, H-8) and 1.57 (3H, d, *J* = 7.0 Hz, $H_3$-9); $\delta_H$ 4.87 (1H, q, *J* = 7.3 Hz, H-10) and 1.55 (3H, d, *J* = 7.3 Hz, $H_3$-12)]. In the $^{13}C$ NMR spectrum for **1a**, in addition to the aldehyde carbon at $\delta_C$ 180.5 (C-1), two carbonyl carbons appeared at $\delta_C$ 172.8 (C-11) and 170.3 (C-7). A combination of the observations suggested the presence of two Ala-derived units [-NCH($CH_3$)C=O-], which was confirmed by HMBC correlations of H-8/C-7, $H_3$-9/C-7, H-10/C-11, and $H_3$-12/C-11, together with COSY correlations of H-8/$H_3$-9 and H-10/$H_3$-12 (Figure 1). One of the Ala-derived units was assigned at the *N* nucleus of the pyrrole based on a key HMBC cross-peak from H-8 to the pyrrole C-5. Meanwhile, the


https://doi.org/10.1021/acsomega.4c10696
ACS Omega 2025, 10, 13185−13192

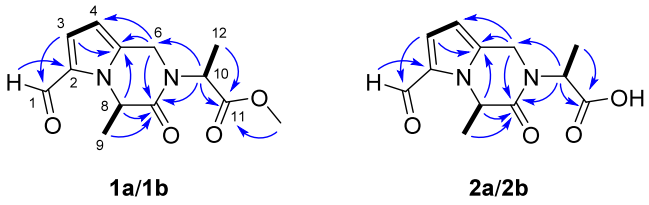


**Figure 1.** Key HMBC (blue arrow) and COSY (thick black line) correlations of **1a**/**1b** and **2a**/**2b**.

downfield methylene protons ($H_2$-6) showed HMBC correlations with the pyrrole C-4 and C-5, as well as the Ala-derived unit carbonyl C-7. Moreover, the methine proton (H-10) of the other Ala-derived unit was analyzed to have HMBC correlations with C-6 and C-7, while a methoxy group [$\delta_H$ 3.71/$\delta_C$ 53.1 (COO*Me*)] showed an HMBC correlation with C-11. These HMBC correlation data indicated that a pyrazinone fused to the pyrrole is present along with a methyl ester of one Ala-derived unit. Thus, the structure of **1a** was determined as the new methyl 2-(6-formyl-4-methyl-3-oxo-3,4-dihydropyrrolo[1,2-*a*]pyrazin-2(1*H*)-yl)propanoate.

The molecular formula for compound **1b** was established to be $C_{13}H_{16}O_4N_2$, the same as **1a**, based on HRESIMS data ([M + H]$^+$ ion at *m*/*z* 265.1178, calcd. 265.1183). Compound **1b** exhibited closely comparable $^1$H and $^{13}$C NMR data with **1a**, except for a few signal shifts ("Manual analysis" in Table 1). The migration of chemical shifts of $\delta_H$ +0.21/$\delta_C$ −1.4 ppm were observed for the C-10 methine [$\delta_H$ 5.08 (1H, q, *J* = 7.4 Hz)/$\delta_C$ 54.2]. In addition, the chemical shift difference between two geminal protons of the downfield methylene [$\delta_H$ 4.73 (1H, d, *J* = 16.5 Hz, H-6a) and 4.67 (1H, br d, *J* = 16.5 Hz, H-6b)] was found to be smaller in **1b** compared to **1a** ($\Delta\delta_{H\text{-}6a\text{-}H\text{-}6b}$ 0.06 ppm in **1b**; 0.09 ppm in **1a**). Taking these subtle changes into consideration, compound **1b** was identified to have the same planar structure as **1a**, which was further supported by an analysis of the $^1$H−$^1$H COSY and $^1$H−$^{13}$C HMBC correlation data (Figure 1).

To address the stereochemistry of **1a** and **1b**, we first considered a plausible mechanism for their formation: the introduction of another L-H-Ala-OMe is presumed to occur later than the formation of a lactone-fused pyrrole structure (Figure S1, Supporting Information). Given the use of chiral substrate L-H-Ala-OMe in the synthetic preparation, C-10 retains the *S* configuration. The stereocenter C-8, on the other hand, is likely to be racemized because the condensation reaction in the modified Maillard reaction between glucose and amine plausibly undergoes the formation of enamine intermediates.[29] Collectively, compounds **1a** and **1b** are stereoisomers that differ in their C-8 absolute configuration.

Electronic circular dichroism (ECD) spectroscopy was employed to determine the C-8 absolute configuration of **1a** and **1b**. Compound **1a** showed opposite signals to **1b** including the ECD Cotton effect near 300 nm (**1a**: positive; **1b**: negative, Figure 2), which was previously reported to be critical for determining the absolute configuration of C-8 in pyrrolooxazinones.[31] Bearing the observation in mind, the ECD curves of (8*S*,10*S*)- and (8*R*,10*S*)-isomers were calculated at the TDDFT/B3LYP/6−31+G(d,p) level using the polarizable continuum model (PCM) solvation model for MeOH. Comparisons of experimental and calculated spectroscopic data showed that the ECD spectrum of **1a** closely agreed with the calculation for the (8*S*,10*S*)-isomer, while that

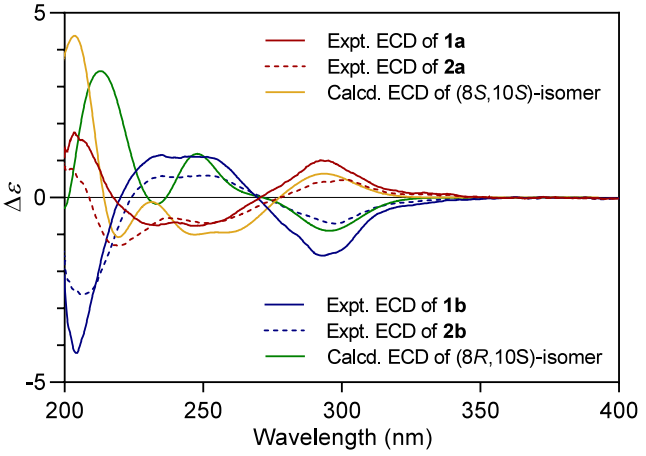


**Figure 2.** Comparison of experimental and calculated ECD spectra for four pyrrolopyrazinones.

of **1b** agreed with the calculation for the (8*R*,10*S*)-isomer. These results were also consistent with the previous report for pyrrolooxazinones where positive Cotton effects near 300 nm indicated 8*S* configuration.[31] Therefore, the absolute configurations of **1a** and **1b** were determined to be (8*S*,10*S*) and (8*R*,10*S*), respectively.

In this study, methyl esters **1a** and **1b** were further hydrolyzed to obtain carboxylic acids **2a** and **2b**, respectively (Scheme 1), for comparative biological evaluation. Most of the $^1$H and $^{13}$C NMR signals in **2a** and **2b** were similar to those observed for **1a** and **1b**, respectively, except for the absence of the methoxy group resonances. The HRESIMS experiments supported the molecular formula $C_{12}H_{14}O_4N_2$ ([M + H]$^+$ ions at *m*/*z* 251.1022, calcd. 251.1026). In addition, compounds **2a** and **2b** showed ECD spectra that closely matched **1a** and **1b**, respectively, indicating that the absolute configuration was conserved upon hydrolysis (Scheme 1 and Figure 2).

**3.2. Long-Range Couplings and HiFSA Analysis.** Upon further examination of the $^1$H NMR spectra of pyrrolopyrazinones, broad peak shapes were observed, particularly at the H-4, H-6a, H-6b, and H-8 resonances (the case of **1a** shown in Figure 3A). To improve peak splitting resolution, Lorentzian−Gaussian windows function (LB −1.2 Hz, GF 0.12) was applied in postacquisition processing, revealing triplet-like peak patterns.[32] Starting with the most significant observation from H-6a ($\delta_H$ 4.77), we endeavored to determine the source of this phenomenon and found that the triple-like peak pattern was appeared by the presence of allylic $^4J$ and homoallylic $^5J$ couplings (Figures 3B and 4).

Improved peak resolution from the postacquisition processing revealed the presence of long-range coupling, but precise determination of the coupling constants remained difficult. Thus, we further employed the QM-HiFSA to fully examine the long-range coupling constants in **1a** and **1b** (Figure 4). The allylic and homoallylic couplings, which were roughly measurable in the triplet-like peak patterns with values of 0.8 and 1.1 Hz, respectively, from the postacquisition processing (LB −1.2 Hz, GF 0.12), were clearly resolved in the QM-HiFSA with values of −0.95 and 1.03 Hz, respectively (Figure 3). The spectral calculation allowed us to unravel more of the long-range spin−spin interactions along with their precise coupling constants ("QM-HiFSA analysis" in Table 1). The pyrrole H-3 was analyzed to have 4- or 5-bond couplings with H-1, H-6a, and H-6b that could not be unambiguously


https://doi.org/10.1021/acsomega.4c10696
ACS Omega 2025, 10, 13185−13192

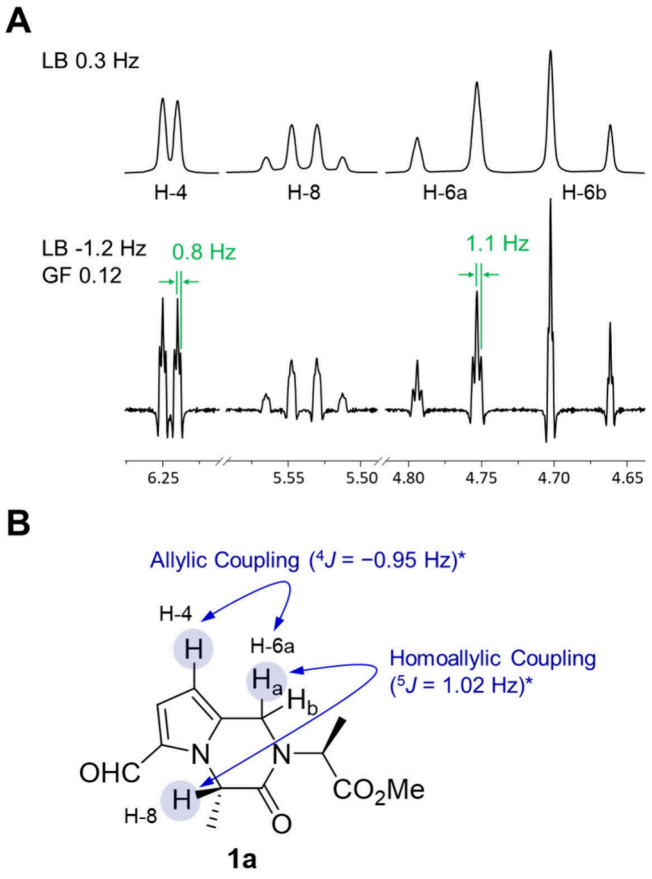


**Figure 3.** (A) Expanded $^1$H NMR spectra of **1a** with different postacquisition processing, exponential multiplication (LB 0.3 Hz, top) and Lorentzian−Gaussian windows function for resolution enhancement (LB −1.2 Hz, GF 0.12, bottom), respectively. (B) Allylic $^4J$ and homoallylic $^5J$ coupling attributable to the triplet-like peak pattern of H-6a in **1a** (*coupling constants were determined by QM-HiFSA analysis).

resolved in any of the postacquisition processing trials performed as long as the quality of the spectral lines was preserved, and the QM-HiFSA with structure-based predictions allowed to deduce the small couplings. Consequently, the careful spectral analysis by the QM-HiFSA methodology in the present study has addressed these subtle but characteristic intramolecular relationships in the pyrrolopyrarinones, which can be used as vital proof for dereplication.

**3.3. Biological Activity Evaluation.** The pharmacological effects previously reported for compounds of the pyrrolopyrazinone class[2−6] motivated the investigation of the biological effects of the four new pyrrolopyrazines in this study. In particular, inspired by their structural similarity to Ranirestat, a potent aldose reductase inhibitor being developed for the treatment of diabetic neuropathy,[15] the aldose reductase inhibitory activities of the four compounds were tested. The reported criticality of carboxyl functional groups in the development of small molecule aldose reductase inhibitors has further rationalized the biological evaluation of these compounds.[15−17] The relative enzyme inhibition activities were compared to that of the control group without compound treatment (DMSO). Interestingly, the four compounds exerted moderate inhibitory effects, with the most values ranging from 5 to 15% over the control group (Table 2). Among them, compound **2a** was found to have the highest inhibitory effect, especially at the tested concentration of 50 $\mu$M (15.30 ± 3.12% inhibition of enzyme activity). Regarding their stereochemical effects, the 8*S*-configured compounds (i.e., compounds **1a** and **2a**) showed relatively higher inhibitory effects than the 8*R*-configured compounds (i.e., compounds **1b** and **2b**). However, the aldose reductase inhibitory activity of these new pyrrolopyrazinone derivatives was weak compared to the positive control, Epalestat, which showed an inhibitory effect of 74.97 ± 1.25% at 100 $\mu$M.

Further, the effect of the compounds on the proliferation of human adipose-derived mesenchymal stem cells (hADMSCs) was evaluated using a CCK-8 assay, to determine the potential

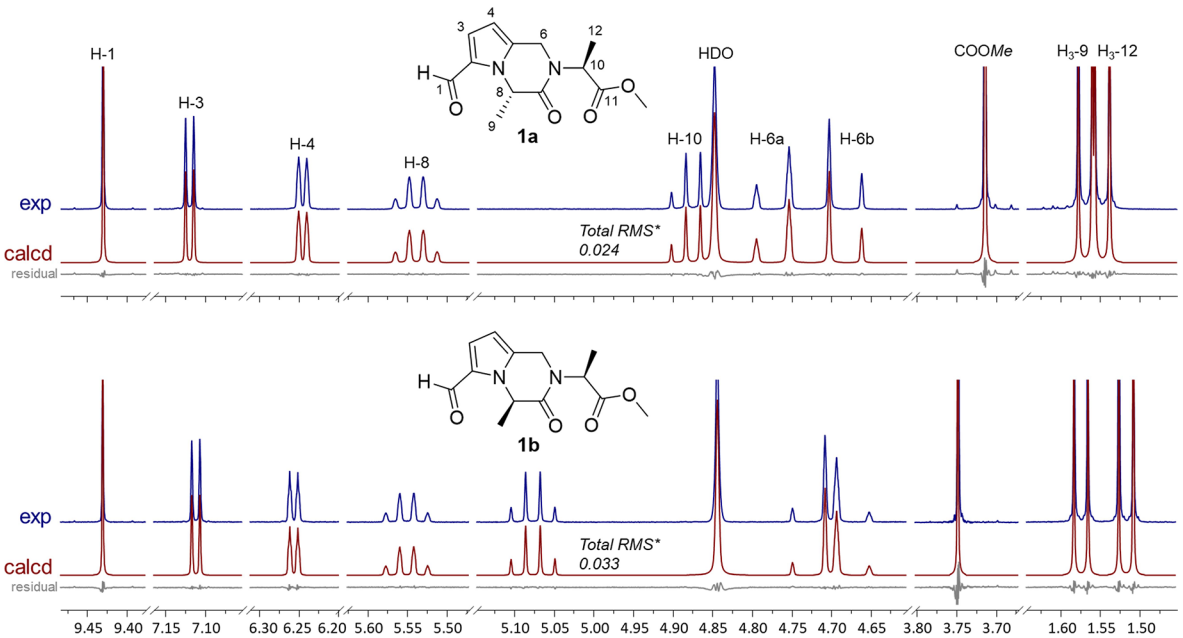


**Figure 4.** QM-HiFSA profiles of **1a** and **1b**: comparison of experimental (exp, blue) and calculated (calcd., red) $^1$H NMR spectra with residuals (*total root−mean−square (RMS) indicates the similarity degree between calculated and experimental spectra).



https://doi.org/10.1021/acsomega.4c10696
ACS Omega 2025, 10, 13185−13192

Table 2. Effect of Aldose Reductase Inhibition Activity of Pyrrolopyrazinones (Mean ± SD, n = 3)

| | % Inhibition | | | | |
|---|---|---|---|---|---|
| concentration ($\mu$M) | DMSO[a] | 1a | 2a | 1b | 2b |
| 25 | 0.00 ± 0.14 | 13.84 ± 0.87 | 8.60 ± 4.89 | 5.11 ± 2.53 | 10.87 ± 0.89 |
| 50 | | 12.71 ± 1.44 | 15.30 ± 3.12 | 8.34 ± 2.89 | 9.26 ± 7.76 |

[a]Negative control.

of these compounds to synergistically treat diabetes-induced cell damage.[23] As a result, the four compounds were found to promote cell proliferation at the concentration of 50 $\mu$M compared to the control (DMSO). Among them, compound **2a**, which had the highest aldose reductase inhibitory activity at 50 $\mu$g/mL, showed the cell proliferative effect with an increase in cell number of 108.41 ± 8.05% after 2 days of culture (**1a**, 105.9 ± 3.51%; **2a**, 108.41 ± 8.05%; **1b**, 111.62 ± 2.30%; **2b**, 113.99 ± 5.23%).

## 4. CONCLUSIONS

In the present study, two previously undescribed pyrolopyrazinones were obtained from the modified Maillard reaction of D-glucose with L-Ala. Subsequential hydrolysis of the methyl ester to the carboxylic acid yielded two additional pyrrolopyrazinones. The interesting feature of their $^1$H NMR spectra was the broad peak shapes (particularly at the H-4, H-6a, H-6b, and H-8 resonances), which are difficult to fully interpret by conventional manual analysis due to their small coupling values. An adjustment of the window function enhanced the resolution of the peak component, and computer-assisted spectral calculations allowed accurate coupling constants to be extracted from the actual experimental data. The complete study of the parameters that primarily record a $^1$H NMR spectrum, i.e., chemical shifts, coupling constants, and line widths, is considered important because it accurately describes the structural information embedded in the spectroscopic data and also allows fast and accurate dereplication in future studies.

The biological evaluation of the pyrrolopyrazinones in this study was inspired by their structural elements. The pyrrolopyrazinones partially share the core structure of Ranirestat, the potent aldose reductase inhibitor, so the biological activity evaluation was directed to the treatment of diabetes. The direction of our biological activity studies was further supported by previous studies on aldose reductase inhibitors with carboxyl functional groups. In the context of the expectation, all of the four compounds showed inhibitory effects, but they were moderate. In addition, the effects of pyrrolopyrazinones on cell proliferation of hADMSCs were evaluated. The rationale was that most of the progressive symptoms of diabetes are related to cell damage. Therefore, the cell proliferation effects of the pyrrolopyrazinones were expected to be synergistic with their aldose reductase inhibitory effects in the diabetes treatment.

## ■ ASSOCIATED CONTENT

### Supporting Information

The Supporting Information is available free of charge at https://pubs.acs.org/doi/10.1021/acsomega.4c10696.

Plausible mechanism for the formation and 1D,2D NMR and HRESIMS data of pyrrolopyrazinones (PDF)

## ■ AUTHOR INFORMATION


### Corresponding Authors

**Jee-Heon Jeong** − *Department of Precision Medicine, School of Medicine, Sungkyunkwan University, Suwon, Gyeonggi 16419, South Korea*; Email: jeeheon@skku.edu

**Joo-Won Nam** − *College of Pharmacy and Core Research Support Center for Natural Products and Medical Materials, Yeungnam University, Gyeongsan, Gyeongbuk 38541, South Korea*; orcid.org/0000-0001-5502-0736; Email: jwnam@yu.ac.kr

### Authors

**Yun-Seo Kil** − *College of Pharmacy, Yeungnam University, Gyeongsan, Gyeongbuk 38541, South Korea; College of Pharmacy and Inje Institute of Pharmaceutical Sciences and Research, Inje University, Gimhae, Gyeongnam 50834, South Korea*

**Junhyeung Park** − *Department of Precision Medicine, School of Medicine, Sungkyunkwan University, Suwon, Gyeonggi 16419, South Korea*

**Byeong-Seon Jeong** − *College of Pharmacy, Yeungnam University, Gyeongsan, Gyeongbuk 38541, South Korea*; orcid.org/0000-0002-7814-6638

**Punam Thapa** − *College of Pharmacy, Yeungnam University, Gyeongsan, Gyeongbuk 38541, South Korea*

**Young Jun Ok** − *Core Research Support Center for Natural Products and Medical Materials, Yeungnam University, Gyeongsan, Gyeongbuk 38541, South Korea*

**Hyukjae Choi** − *College of Pharmacy, Yeungnam University, Gyeongsan, Gyeongbuk 38541, South Korea*

Complete contact information is available at: https://pubs.acs.org/10.1021/acsomega.4c10696


### Author Contributions

All authors have approved the final version of the manuscript

### Notes

The authors declare no competing financial interest.

## ■ ACKNOWLEDGMENTS

This research was supported by Basic Science Research Program through the National Research Foundation of Korea (NRF), funded by the Ministry of Science and ICT (MSIT) (NRF-2022R1A2C1009496), and the Ministry of Education (RS-2023-00240669). This research was also supported by Korea Basic Science Institute (National Research Facilities and Equipment Center) grant funded by the Ministry of Education (grant No. 2019R1A6C1010046). The authors sincerely thank Mr. Matthias Niemitz (NMR Solutions Ltd., Kuopio, Finland) for providing support with HiFSA computations using Cosmic Truth. The authors also thank the Core Research Support Center for Natural Products and Medical Materials (CRCNM) for technical support regarding 600 MHz NMR, CD-ORD, and HRESIMS.

## REFERENCES


(1) Bhardwaj, V.; Gumber, D.; Abbot, V.; Dhiman, S.; Sharma, P. Pyrrole: A resourceful small molecule in key medicinal hetero-aromatics. *RSC Adv.* **2015**, *5* (20), 15233−15266.

(2) D'Ambrosio, M.; Guerriero, A.; Debitus, C.; Ribes, O.; Pusset, J.; Leroy, S.; Pietra, F. Agelastatin A, a new skeleton cytotoxic alkaloid of the oroidin family. Isolation from the axinellid sponge *Agelas dendromorpha* of the Coral Sea. *J. Chem. Soc., Chem. Commun.* **1993**, No. 16, 1305−1306.

(3) Cafieri, F.; Fattorusso, E.; Mangoni, A.; Taglialetela-Scafati, O. Longamide and 3,7-dimethylisoguanine, two novel alkaloids from the marine sponge *Agelas longissima*. *Tetrahedron Lett.* **1995**, *36* (43), 7893−7896.

(4) Uemoto, H.; Tsuda, M.; Kobayashi, J. i. Mukanadins A-C, new bromopyrrole alkaloids from marine sponge *Agelas nakamurai*. *J. Nat. Prod.* **1999**, *62* (11), 1581−1583.

(5) Jansen, R.; Sood, S.; Mohr, K. I.; Kunze, B.; Irschik, H.; Stadler, M.; Mueller, R. Nannozinones and sorazinones, unprecedented pyrazinones from *Myxobacteria*. *J. Nat. Prod.* **2014**, *77* (11), 2545−2552.

(6) Zhu, Y.; Wang, Y.; Gu, B.-B.; Yang, F.; Jiao, W.-H.; Hu, G.-H.; Yu, H.-B.; Han, B.-N.; Zhang, W.; Shen, Y.; et al. Antifungal bromopyrrole alkaloids from the South China Sea sponge *Agelas* sp. *Tetrahedron* **2016**, *72* (22), 2964−2971.

(7) Casuscelli, F.; Ardini, E.; Avanzi, N.; Casale, E.; Cervi, G.; D'Anello, M.; Donati, D.; Faiardi, D.; Ferguson, R. D.; Fogliatto, G.; et al. Discovery and optimization of pyrrolo[1,2-a]pyrazinones leads to novel and selective inhibitors of PIM kinases. *Bioorg. Med. Chem.* **2013**, *21* (23), 7364−7380.

(8) Trushkov, I. V.; Nevolina, T. A.; Shcherbinin, V. A.; Sorotskaya, L. N.; Butin, A. V. Furan ring opening-pyrrole ring closure. A simple route to 1,2,3,4-tetrahydropyrrolo[1,2-a]pyrazin-3-ones. *Tetrahedron Lett.* **2013**, *54* (30), 3974−3976.

(9) Shiokawa, Z.; Inuki, S.; Fukase, K.; Fujimoto, Y. Efficient synthesis of (−)-hanishin, (−)-longamide B, and (−)-Longamide B methyl ester through piperazinone formation from 1,2-cyclic sulfamidates. *Synlett* **2016**, *27* (4), 616−620.

(10) Shiokawa, Z.; Kashiwabara, E.; Yoshidome, D.; Fukase, K.; Inuki, S.; Fujimoto, Y. Discovery of a novel scaffold as an indoleamine 2,3-dioxygenase 1 (IDO1) inhibitor based on the pyrrolopiperazinone alkaloid, longamide B. *ChemMedChem.* **2016**, *11* (24), 2682−2689.

(11) Yan, L.-J. Redox imbalance stress in diabetes mellitus: Role of the polyol pathway. *Animal Model Exp. Med.* **2018**, *1* (1), 7−13.

(12) Wu, J.; Jin, Z.; Zheng, H.; Yan, L.-J. Sources and implications of NADH/NAD+ redox imbalance in diabetes and its complications. *Diabetes, Metab. Syndr. Obes.: Targets Ther.* **2016**, *9*, 145−153.

(13) Ramana, K. V.; Srivastava, S. K. Aldose reductase: A novel therapeutic target for inflammatory pathologies. *Int. J. Biochem. Cell Biol.* **2010**, *42* (1), 17−20.

(14) Jannapureddy, S.; Sharma, M.; Yepuri, G.; Schmidt, A. M.; Ramasamy, R. Aldose Reductase: An emerging target for development of interventions for diabetic cardiovascular complications. *Front. Endocrinol.* **2021**, *12*, No. 636267.

(15) Negoro, T.; Murata, M.; Ueda, S.; Fujitani, B.; Ono, Y.; Kuromiya, A.; Komiya, M.; Suzuki, K.; Matsumoto, J.-i. Novel, highly potent aldose reductase inhibitors: (*R*)-(−)-2-(4-Bromo-2-fluorobenzyl)-1,2,3,4-tetrahydropyrrolo[1,2-*a*]pyrazine- 4-spiro-3′-pyrrolidine-1,2′,3,5′-tetrone (AS-3201) and its congeners. *J. Med. Chem.* **1998**, *41* (21), 4118−4129.

(16) Qin, X.; Hao, X.; Han, H.; Zhu, S.; Yang, Y.; Wu, B.; Hussain, S.; Parveen, S.; Jing, C.; Ma, B.; et al. Design and synthesis of potent and multifunctional aldose reductase inhibitors based on quinoxalinones. *J. Med. Chem.* **2015**, *58* (3), 1254−1267.

(17) Singh Grewal, A.; Bhardwaj, S.; Pandita, D.; Lather, V.; Singh Sekhon, B. Updates on aldose reductase inhibitors for management of diabetic complications and non-diabetic diseases. *Mini-Rev. Med. Chem.* **2015**, *16* (2), 120−162.

(18) Napolitano, J. G.; Lankin, D. C.; McAlpine, J. B.; Niemitz, M.; Korhonen, S.-P.; Chen, S.-N.; Pauli, G. F. Proton fingerprints portray molecular structures: Enhanced description of the $^{1}$H NMR spectra of small molecules. *J. Org. Chem.* **2013**, *78* (19), 9963−9968.

(19) Pauli, G. F.; Chen, S.-N.; Lankin, D. C.; Bisson, J.; Case, R. J.; Chadwick, L. R.; Godecke, T.; Inui, T.; Krunic, A.; Jaki, B. U.; et al. Essential parameters for structural analysis and dereplication by $^{1}$H NMR spectroscopy. *J. Nat. Prod.* **2014**, *77* (6), 1473−1487.

(20) Achanta, P. S.; Jaki, B. U.; McAlpine, J. B.; Friesen, J. B.; Niemitz, M.; Chen, S.-N.; Pauli, G. F. Quantum mechanical NMR full spin analysis in pharmaceutical identity testing and quality control. *J. Pharm. Biomed. Anal.* **2021**, *192*, No. 113601.

(21) Tang, Y.; Friesen, J. B.; Lankin, D. C.; McAlpine, J. B.; Nikolic, D.; Chen, S.-N.; Pauli, G. F. Geraniol-derived monoterpenoid glucosides from *Rhodiola rosea*: resolving structures by QM-HifSA methodology. *J. Nat. Prod.* **2023**, *86* (2), 256−263.

(22) Kil, Y.-S.; Nam, J.-W. Quantum-mechanical driven $^{1}$H iterative full spin analysis addresses complex peak patterns of choline sulfate. *ACS Omega* **2022**, *7* (46), 42607−42612.

(23) Huang, Q.; Huang, Y.; Liu, J. Mesenchymal stem cells: An excellent candidate for the treatment of diabetes mellitus. *Int. J. Endocrinol.* **2021**, *2021*, No. 9938658.

(24) Kil, Y.-S.; Baral, A.; Jeong, B.-S.; Laatikainen, P.; Liu, Y.; Han, A.-R.; Hong, M.-J.; Kim, J.-B.; Choi, H.; Park, P.-H.; et al. Combining NMR and MS to describe pyrrole-2-carbaldehydes in wheat bran of radiation. *J. Agric. Food Chem.* **2022**, *70* (40), 13002−13014.

(25) Shao, Y.; Molnar, L. F.; Jung, Y.; Kussmann, J.; Ochsenfeld, C.; Brown, S. T.; Gilbert, A. T. B.; Slipchenko, L. V.; Levchenko, S. V.; O'Neill, D. P.; et al. Advances in methods and algorithms in a modern quantum chemistry program package. *Phys. Chem. Chem. Phys.* **2006**, *8* (27), 3172−3191.

(26) *Gaussian 16*; Gaussian, Inc.: Wallingford, CT, 2016.

(27) *SpecDis*; Berlin, Germany, 2017. https:/specdis-software.jimdo.com .

(28) Hong Bui, H. T.; Uprety, A.; Ngo, T. H.; Kil, Y.-S.; Thapa, P.; Mo, J.; Choi, H.; Kim, S. Y.; Nam, J.-W. Quantum-mechanics-based structural analysis of phenolic glycosides from *Cuscuta japonica* seeds with protective effects against $H_2O_2$-induced oxidative stress in SH-SY5Y cells. *Phytochemistry* **2025**, *234*, 114420.

(29) Adhikary, N. D.; Kwon, S.; Chung, W.-J.; Koo, S. One-pot conversion of carbohydrates into pyrrole-2-carbaldehydes as sustainable platform chemicals. *J. Org. Chem.* **2015**, *80* (15), 7693−7701.

(30) Li, J.; Pan, L.; Naman, C. B.; Deng, Y.; Chai, H.; Keller, W. J.; Kinghorn, A. D. Pyrrole alkaloids with potential cancer chemopreventive activity isolated from a goji berry-contaminated commercial sample of African mango. *J. Agric. Food Chem.* **2014**, *62* (22), 5054−5060.

(31) Wang, P.; Kong, F.; Wei, J.; Wang, Y.; Wang, W.; Hong, K.; Zhu, W. Alkaloids from the mangrove-derived actinomycete *Jishengella endophytica* 161111. *Mar. Drugs* **2014**, *12* (1), 477−490.

(32) McAlpine, J. B.; Chen, S.-N.; Kutateladze, A.; MacMillan, J. B.; Appendino, G.; Barison, A.; Beniddir, M. A.; Biavatti, M. W.; Bluml, S.; Boufridi, A.; et al. The value of universally available raw NMR data for transparency, reproducibility, and integrity in natural product research. *Nat. Prod. Rep.* **2019**, *36* (1), 35−107.




https://doi.org/10.1021/acsomega.4c10696
*ACS Omega* 2025, 10, 13185−13192